Pre-turbo After-treatment System Development using a 1D Modeling Approach

ABSTRACT

The location of a diesel engine's after-treatment system can dramatically affect engine performance. A numerical study was conducted to verify that impact in relation to engine performance. A part of that investigation included examining the advantages and disadvantages of locating the after-treatment system before or after the turbocharger. The operating conditions that were used to conduct the testing included both steady-state and transient conditions. Two key after-treatment devices included in the tests were a Diesel Oxidation Catalyst (DOC), which was then followed directly downstream by a Diesel Particulate Filter (DPF). Experiments obtained the individual, pressure drop and warm-up data sets for each of the DOC and DPF models that were used. One additional step was taken for the transient studies, which modeled the chemical reactions within the DOC to simulate HC and CO oxidation, and their associated exothermic behavior.

The results showed that fuel economy was improved under steady-state conditions with a pre-turbo after-treatment system as opposed to a post-turbo system. However, this advantage is minimal for a relatively unloaded DPF after-treatment system. Operating under transient conditions provided less impressive response times for a pre-turbo after-treatment system. The transient behavior of the pre-turbo system did improve somewhat with exothermic chemical reactions in the DOC, but not enough to overcome the large thermal inertia of the DP, which compounds the problem.

INTRODUCTION

Automotive manufacturers and suppliers are presented with the task of trying to meet increasingly strict emissions regulations, while still being profitable and staying ahead of their competition in the marketplace. Due in part to increased regulations, exhaust gas after-treatment systems are now an integral part of the modern diesel powertrain. To control the emissions of oxides of nitrogen, significant levels of Exhaust Gas Recirculation (EGR) are required. Increasing the EGR operation increases the levels of particulate matter, which then requires additional countermeasures. Reducing the levels of particulate matter is accomplished with the addition of a Diesel Particulate Filter (DPF). These filters are usually Cordierite or Silicone Carbide monoliths. These two filter types have unique cost and performance advantages, as well as separate manufacturing protocols. The Diesel Oxidation Catalyst (DOC) oxidizes gaseous and liquid hydrocarbons along with carbon monoxide. Typically, a DOC is composed of a canister filled with a honeycomb substrate. The honeycomb configuration of the substrate offers a large surface area that is coated with precious metals such as platinum or palladium. The precious metals used in the substrate act as catalysts for oxidation reactions.

Based on the viewpoint of gas dynamics, an after-treatment system restricts the exhaust. In terms of performance, any device that adds exhaust back pressure is detrimental, because it reduces the net mean effective pressure available from the engine. This adds further complexity because the loading of a DPF changes over time, which results in fluctuations in available engine power. Consequently, it is important to minimize the negative back-pressure of any after-treatment system.

A significant impact can be made on steady state and transient engine performance through the optimum location of and after-treatment system within the exhaust system of a turbocharged diesel engine. Investigations into the relative advantages and disadvantages are crucial for locating the after-treatment system before or after the turbine. The primary purpose of this study is to quantify the consequences of steady-state and transient performance on after-treatment systems placed before and after the exhaust gas turbine. Prior to examining the pros and cons of placement from a thermodynamic viewpoint, it is crucial to study the physical impacts as well. Putting the after-treatment system in front of the turbocharger adds tremendous physical stress on these emissions reduction devices. A pre-turbo placement of after-treatment systems exposes the DOC and DPF pressure and temperature conditions that are significantly higher than if they were placed after the turbocharger. Therefore, challenges are presented for this system in relation to durability and its consequences for service / replacement intervals. Additional expense occurs with the potential need for materials with the capacity to handle higher pressure and temperature tolerances that will permit this system to operate in the pre-turbo environment.

METHODOLOGY

ENGINE MODEL - The engine candidate featured in this study is a 1.9L, 4-cylinder, DI diesel engine equipped with a Variable Geometry Turbocharger (VGT). The engine model is configured to enable both high pressure and low pressure Exhaust Gas Recirculation (EGR). PID-style electronic controllers are setup to allow precise control of boost pressure, and EGR concentration. The model was calibrated with engine dynamometer test data.

DOC MODEL – The DOC model is based on an existing series-production catalyst. It is an Emitec product with a round 1.4L metallic substrate of dimensions D x L of 4.65" x 5" (Type 200/400 LS/PE). DOC pressure loss behavior and thermal mass was calibrated against experimentally-obtained thermodynamic data. DOC chemistry in terms of CO and HC conversion efficiency was calibrated against experimentally-obtained species concentration data.

DPF MODEL – The DPF model is based on an existing production particulate filter. It is an NGK product with D x L of 5.66" x 6". The substrate (MSC111) has a porosity of 52%, cell density of 300 CPSI and wall thickness of 12 mil. DPF pressure drop was calibrated against published cold flow measurements. Thermal mass was calibrated against experimentally-obtained thermodynamic data.

BOUNDARY CONDITIONS

Steady state operating points are listed below:
1. 1500 r/min, 2, 4, 6, 8, 10, 12, 14, 16 bar BMEP and three DPF loading states
2. 2500 r/min, 2, 4, 6, 8, 10, 12, 14, 16 bar BMEP and three DPF loading states
3. 4000 r/min, 2, 4, 6, 8, 10, 12, 14, 16 bar BMEP and three DPF loading states

For operating points 1, 2 and 3, VGT rack position control and fueling control was employed to achieve the target BMEP levels. A lambda limit based on engine dynamometer test data was set to avoid unrealistic fueling. At certain VGT rack positions, the target BMEP is not achievable under higher DPF loading states. BMEP that is achieved varies with the PMEP consequence of the after-treatment system location and DPF state of loading. The three loading conditions can be characterized by the pressure drop across the DPF at the 4000 r/min, 12 bar BMEP operating point. These loading conditions are shown in Table 1 below:

Loading condition (-)	**Pressure drop across DPF (mbar)**
Clean	200
Moderate	300
High	800

Table 1: DPF Loading and Corresponding Pressure Drop

Transient operating points are listed below:
1500 r/min, 2 to 16 bar BMEP load step for the following three cases:
1. Baseline with no after-treatment system
2. Pre-turbine after-treatment system
3. Post-turbine after-treatment system

MODEL CORRELATION

DPF MODEL PRESSURE DROP AND THERMAL MASS CORRELATION - DPF pressure drop is calibrated through specification of permeability and the so-called Forchheimer constant for the substrate wall. Figure 1 shows the DPF pressure drop at different mass flow rates, under cold flow conditions. The results predicted by the GT-Power model correlate with data published in the literature [6].

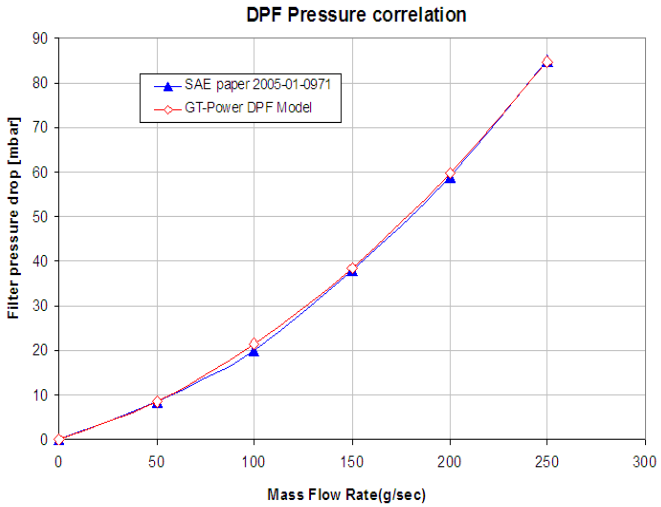

Figure1: Results from DPF Pressure Drop Correlation

DPF warm up calibration is performed by specifying the packing density of the filter substrate. Experimental data providing mass flow rate, as well as inlet and outlet temperature histories for the DPF were used for this warm-up correlation effort. The measured DPF inlet mass flow rate and temperature history is prescribed, and the density of the filter substrate is varied gradually until DPF outlet temperature predictions match measurements.

Figure 2 shows the DPF warm-up calibration results. The experimental DPF in and out temperatures have a difference during steady-state due to heat loss to the surroundings. The model does not consider this heat loss and assumes that at steady-state the DPF out temperature approaches the DPF in temperature. The DPF out temperature predicted by the GT-Power model during the warm-up period (first 200 seconds) is nearly identical to the experimental data. The correlated DPF model was used in the engine transient response studies (these transients were all less than 200 sec in duration).

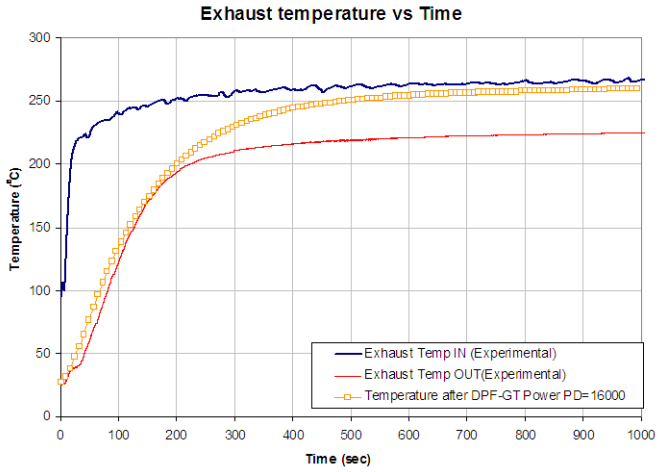

Figure 2: Results from DPF Thermal Mass Correlation

DOC MODEL PRESSURE DROP AND THERMAL MASS CORRELATION - DOC pressure drop is correlated using a series of orifices placed downstream of the DOC. The pressure drop through this series of restrictions mimics the pressure drop behavior of the DOC.

Figure 3 shows the DOC pressure drop for varying exhaust mass flow rates. It can be seen that correlation efforts were successful at capturing the pressure loss behavior as measured experimentally.

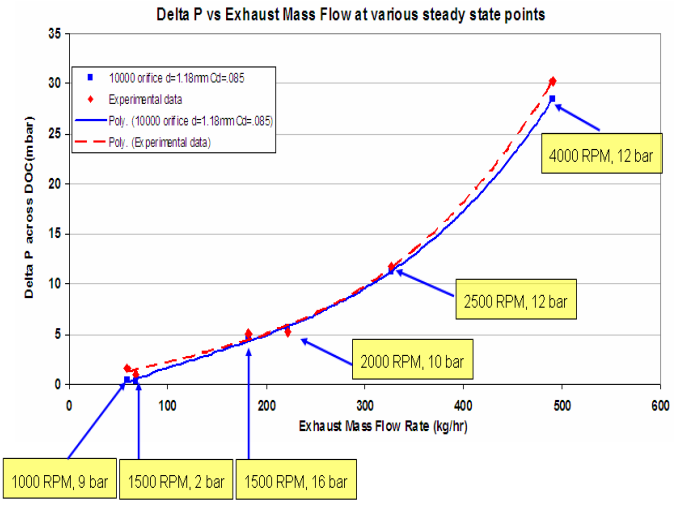

Figure 3: Results of DOC Pressure Drop Correlation

DOC warm up was modeled with two distinct approaches. In the first approach, a 'thermal pipe' object is used to model the substrate and canister mass. Heat transfer coefficients representing heat transfer from the exhaust gas to the canister and from the canister to the external environment are calibrated to match experimental warm up data for the DOC. Figure 4 depicts this approach. Figure 5 shows that the DOC outlet temperature predicted by the model is nearly identical to the measured data. The model was also executed adiabatically, or in other words, without considering heat loss to the environment. This assumption ensures that at a steady-state, the DOC outlet temperature equals the DOC inlet temperature (also shown in figure 5).

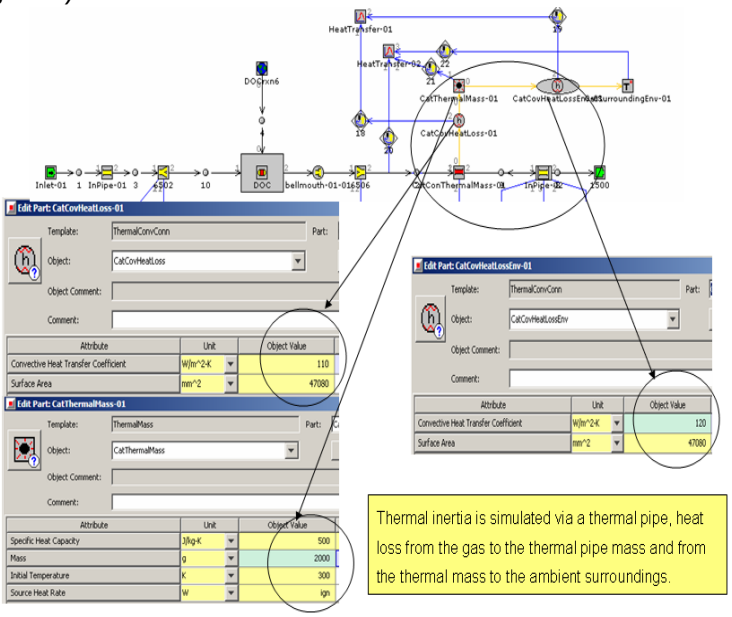

Figure 4: DOC Warm-up Correlation ('Thermal Pipe' Object)

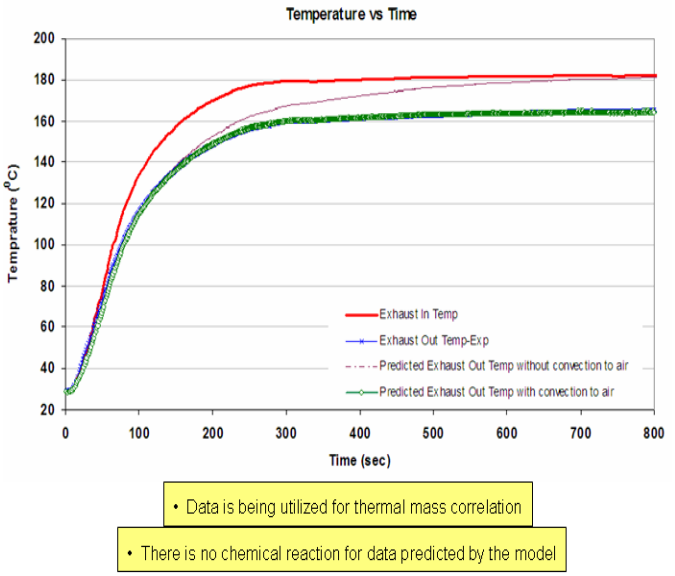

Figure 5: Results of DOC Warm-up Correlation ('Thermal Pipe' Object)

In the second approach, a 'pipe' object is used to model the DOC substrate and canister mass. The heat transfer coefficients representing heat transfer from the exhaust gas to the canister and from the canister to the external environment is calculated by the model. Figure 6 shows that with this approach also, the DOC outlet temperature closely matches that of the experimental data. The model was also executed adiabatically as in the previous approach, so that at steady-state, DOC outlet temperature equals DOC inlet temperature.

All subsequent results discussed in this paper feature the second modeling approach, and do not consider heat transfer from the canister to the external environment (adiabatic).

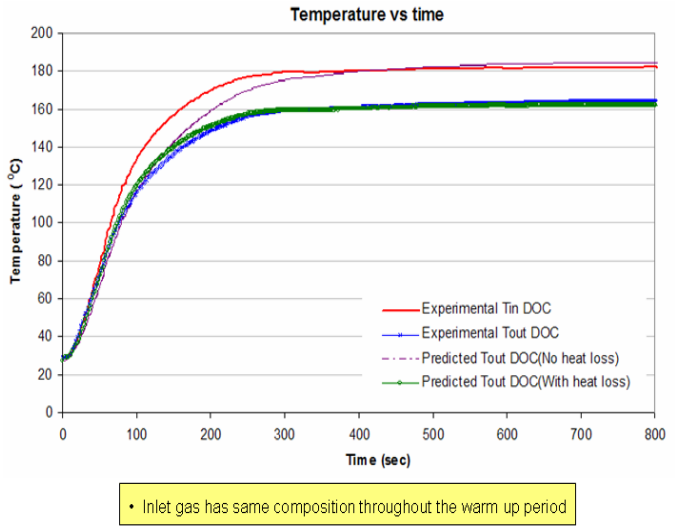

Figure 6: Results of DOC Warm-up Correlation ('Pipe Object')

The adiabatic assumption was selected, because it was discovered that there were unintended external sources of cooling in the test cell setup, which aggravated heat rejection from the outer skins of the DOC and DPF to the external environment at steady-state. This external cooling effect was minimal at lower temperatures (early period of warm-up), becoming more pronounced as the inlet gas temperature increased (i.e. higher temperature difference). It was therefore reasonable to correlate the model to the early warm-up period of the test data, and then allow the model to predict the tail end of the warm-up and subsequent progression into steady-state behavior. It should also be noted that this assumption of adiabatic behavior does not impact the transient results obtained in this study, as these studies are all short enough in duration that they do not go beyond the initial warm-up period where the model correlates well with the measured data. This assumption has an impact on the steady-state results obtained in this study, because the assumption of adiabatic behavior provides for an elevated DPF outlet temperature which corresponds to an elevated turbine inlet temperature in the pre-turbo setup. This provides for slightly higher turbine power. The impact is minimal in the post-turbo configuration.

DOC MODEL CHEMICAL KINETICS SETUP AND CORRELATION - DOC reaction chemistry is modeled using both the global reactions approach as well as the surface reactions approach. Experimental data is available showing DOC inlet and outlet concentrations for CO, HC, and oxygen. Corresponding air and fuel flow rates are also available. The chief objective of the kinetics study was to model CO and hydrocarbon oxidation, and so it is assumed for the sake of simplicity that concentrations of oxides of nitrogen are negligible. Figure 7 depicts the setup of the chemical balance and species concentrations.

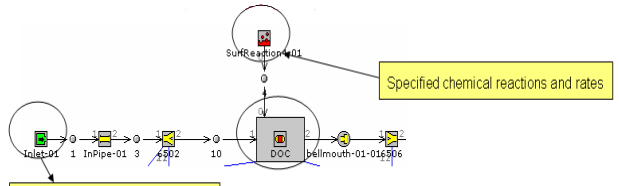

	1	2	3	4	5	6	7	8	9	10	11	12	13	14	15
N2	0.756631	0.754942	0.755243	0.753348	0.753406	0.752967	0.75087	0.744637	0.746711	0.745727	0.742424	0.742891	0.74229	0.742723	0.766001
CO2	0.045761	0.051142	0.050548	0.056877	0.057441	0.059654	0.067467	0.087781	0.082505	0.086602	0.097874	0.097191	0.099628	0.106754	0.11
H2O	0.013756	0.01083	0.012764	0.010626	0.013617	0.016003	0.016644	0.007784	0.016652	0.01886	0.016315	0.02043	0.021711	0.057551	0.06
O2	0.183608	0.182836	0.181181	0.178863	0.175222	0.171029	0.164629	0.159333	0.153595	0.148188	0.142671	0.138699	0.135499	0.091252	0.054729
NO	0	0	0	0	0	0	0	0	0	0	0	0	0	0	0
NO2	0	0	0	0	0	0	0	0	0	0	0	0	0	0	0
H2	0	0	0	0	0	0	0	0	0	0	0	0	0	0	0
CO	0.000203	0.000208	0.000221	0.000239	0.000262	0.000289	0.000332	0.0004	0.000461	0.000538	0.000617	0.000683	0.000754	0.001534	0.008071
C3H8	4.25E-05	4.24E-05	4.44E-05	4.72E-05	5.19E-05	5.79E-05	5.65E-05	6.39E-05	7.52E-05	8.4E-05	9.79E-05	0.000106	0.000117	0.000187	0.001199

The gas composition is estimated according to the equation:

$C_xH_y + z(O_2+3.76\ N_2) \rightarrow p\ CO_2 + a\ CO + b\ O_2 + c\ C_3H_8 + q\ H_2O + 3.76z\ N_2$ and the experimental a, b, c and Air Fuel Ratio data.

The input to the model is in Mass Fraction which is =

Concentration in ppm * 10^{-6} *Molecular weight of the species/ Molecular weight of the exhaust gas

Figure 7: DOC Chemical Kinetics Setup

For both global and surface reactions, Arrhenius equations and inhibition reactions are calibrated to obtain the CO and HC conversion rates seen in the experimental data. All the available experimental data resided within a narrow gas temperature range around 200^o C. As a cross-check, the model was executed in several distinct temperature ranges to verify that a reasonable increase in conversion efficiency is achieved with an increase in gas temperature. Figures 8 and 9 show the CO and HC conversion efficiencies for the global reactions approach. Figures 10 and 11 on the other hand depict the same efficiencies resulting from the surface reactions approach. Figures 8 through 11 also show the effect of increased temperature on the associated species conversion efficiencies.

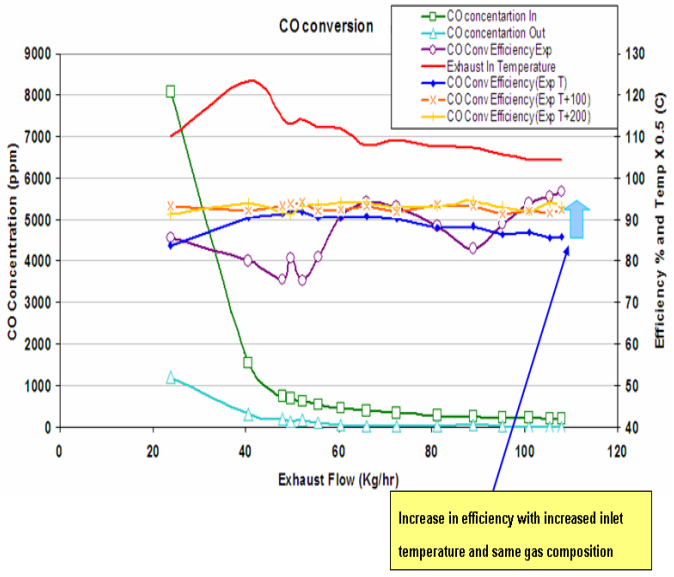

Figure 8: Results of CO Conversion (Global Reactions)

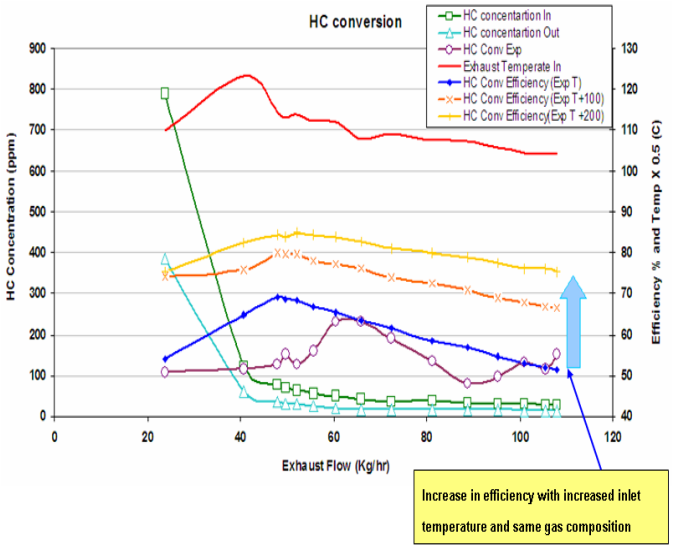

Figure 9: Results of HC Conversion (Global Reactions)

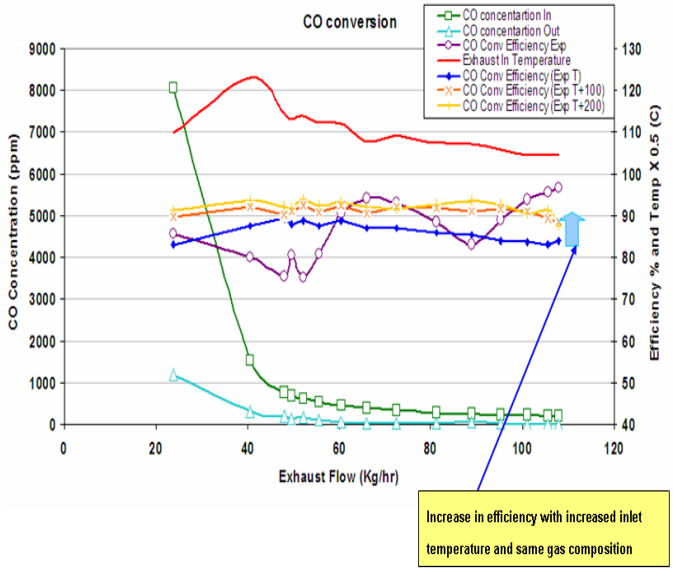

Figure 10: Results of CO Conversion (Surface Reactions)

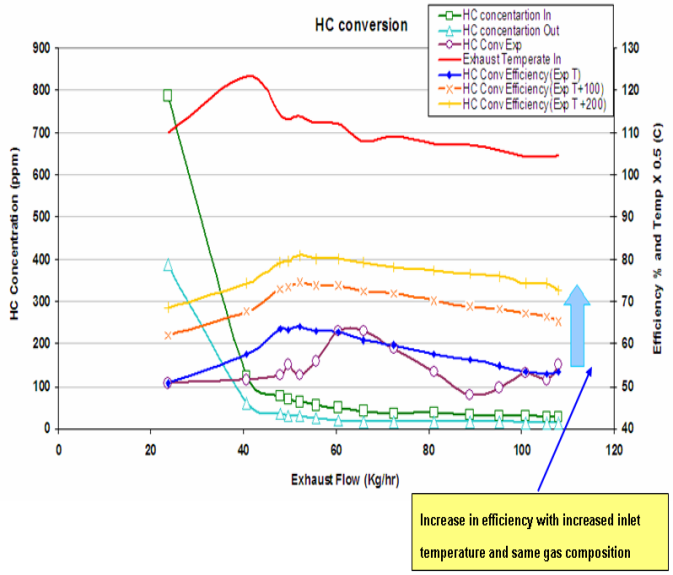

Figure 11: Results of HC Conversion (Surface Reactions)

RESULTS & DISCUSSION

PLACEMENT INVESTIGATIONS

DPF location has a direct impact on engine and turbocharger performance. This is affected by two primary pathways, which are local gas density and impact on turbine expansion ratio.

A post-turbo after-treatment system sees significantly lower gas densities than a pre-turbo after-treatment system. This is because the exhaust gas has already expanded through the turbine in the post-turbo configuration and is at a significantly lower pressure. The gas temperature also decreases but the reduction in pressure is more drastic than the reduction in temperature.

From the ideal gas equation of state $\rho = \frac{P}{R \times T}$, falling pressure results in a density reduction.

The temperature fall dampens this reduction somewhat but pressure changes more significantly. The lower density results in a higher volume flow rate and a consequent increase in pressure drop.

The second influencing factor is the turbine expansion ratio. For simplicity let us assume that the pressure drops are equivalent. This would require the assumption of the same gas densities at the inlet of both after-treatment configurations. If this were done, it might look like comparable performance will be achieved by both engine setups. The pre-turbo setup would see a direct restriction of exhaust ports which would raise the pumping work necessary during exhaust strokes. The post-turbo setup would experience a reduction in expansion ratio, which would then require VGT adjustment to compensate and would then also raise the exhaust port pressures and aggravate pumping work. If this were true, approximately the same PMEP for both configurations is expected because the same pressure drop was experienced in the exhaust system, only at different locations. This, in reality, is not true. A more detailed analysis shows that a post-turbine restriction is far more detrimental than a pre-turbine restriction. To illustrate this, a simple example is used. Let us assume an initial P3 (refer to Figure 12) of say 4 bar, and a nominal P4 of 1 bar for a system with no after-treatment system. The expansion ratio across the turbine is given by P3/P4 which equals 4 in this case. Now let us assume that the pressure drop through the after-treatment system is fixed regardless of where it is placed (i.e. no sensitivity to gas properties). This pressure drop is assumed to be equal to 1 bar. In a pre-turbo configuration, this would have the effect of raising the pumping back pressure from 4 bar to 5 bar. The turbine expansion ratio stays the same. For a post-turbo setup, P4 will be raised to 2 bar. The expansion ratio is now reduced from 4 to 2. This lost expansion ratio can be gained by increasing P3 by 1 bar, With P3 of 5 bar, and P4 of 2 bar, an expansion ratio of only 5/2 or 2.5 can be achieved. In order to get back to the expansion ratio of 4, P3 would have to be increased to 8 bar. That would result in a pumping back pressure of 8 bar. So the same pressure drop of 1 bar results in a 1 bar exhaust back pressure penalty when the after-treatment system is upstream of the turbine, and an extremely significant 4 bar penalty when it is located downstream of the turbine (for the same expansion ratio). Figure 12 is an illustration of this simple example.

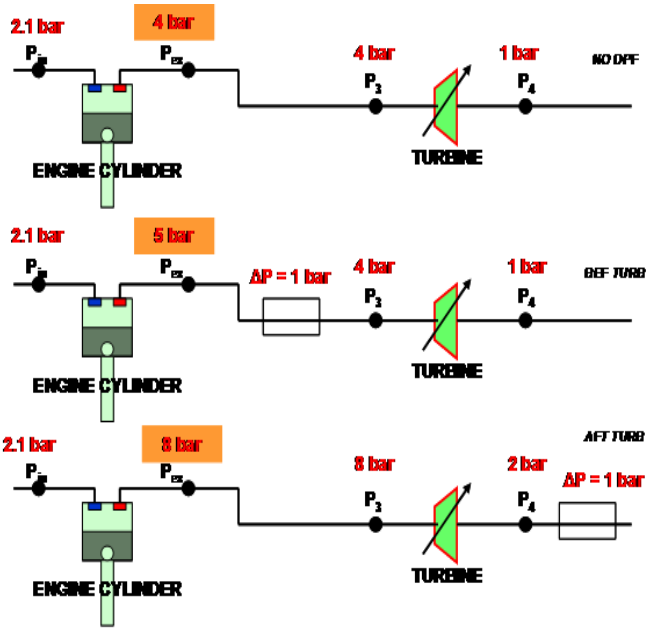

Figure 12: Effect on Turbine Expansion Ratio.

Both of these phenomena show distinct benefits for a pre-turbo DPF system as compared to its post-turbo counterpart. Figure 13 shows the layout of the various system placements studied.

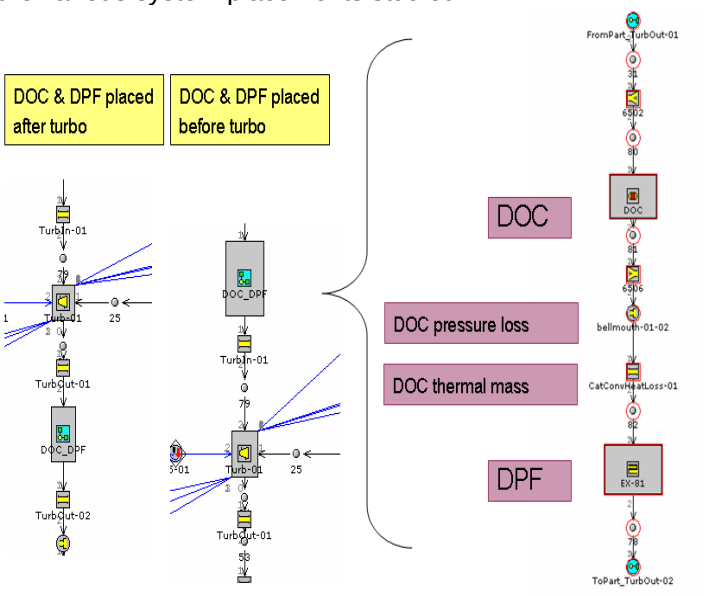

Figure 13: Pre and post-turbine layouts

Steady-state simulations - Steady state performance maps were developed to illustrate the relative fuel consumption benefit of a pre-turbine configuration versus a post-turbine configuration. This was conducted in the context of a highly loaded, moderately loaded, and unloaded (clean) DPF. In the case of the highly loaded DPF, it is observed that the post-turbine configuration sustains a much higher pressure drop across the after-treatment system. This is due to the expansion-ratio reducing effect on the turbine, as well as lower gas density which leads to higher volume flowrates through the after-treatment system. This results in higher pumping losses which in turn aggravates fuel consumption. The models predict up to a 3% fuel efficiency gain for the pre-turbine configuration in comparison to its post-turbine counterpart. The BSFC benefit is mainly observed in high speed, high load operation where the after-treatment system experiences high exhaust flow. At low engine speeds and loads the BSFC benefit is minor.

This gain in fuel efficiency is also reduced as one migrates from a highly loaded DPF to a moderately loaded DPF, and finally to a clean DPF. This is chiefly due to the fact that the pressure loss consequence across the after-treatment systems is reduced as the DPF loading is reduced. This reduces the effect seen with pumping losses and hence, fuel consumption.

The study noted the increase in pressure drop across the highly loaded after-treatment system with increases in engine speed and load. This increase is higher in the post-turbine configuration as compared to the pre-turbine configuration. This results in higher pumping losses for the post-turbine configuration and a consequent penalty in terms of specific fuel consumption.

In comparison to a highly loaded after-treatment system, the pressure drop is much lower. Even then the pressure drop is higher in the post-turbine configuration as compared to the pre-turbine configuration. This again results in higher pumping losses for the post-turbine configuration and a consequent penalty in terms of specific fuel consumption. This effect is observed also in the clean after-treatment system but at a much smaller scale.

Transient simulations – The calibrated after-treatment system comprised of the DOC and DPF is placed prior to, and directly after the turbine to evaluate relative differences in terms of engine transient response. Both systems are compared to the baseline engine model that does not feature any exhaust emissions countermeasures. Figure 14 provides a BMEP history for the baseline, pre-turbine and post- turbine configurations respectively.

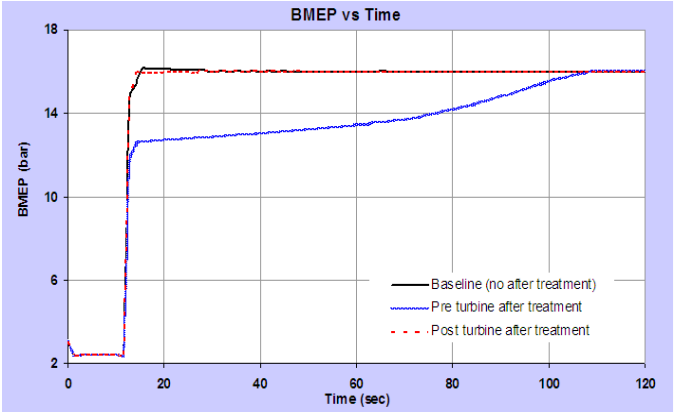

Figure 14: Transient Response for Various Configurations

A constant-speed load step from 1500 rpm, 2 bar BMEP to 16 bar BMEP is commanded. The turbine rack was in its closed position before the load step. Rack position was modulated with a PID controller to achieve 16 bar BMEP. Once the target BMEP of 16 bar is achieved, the rack was opened to maintain 16 bar BMEP during the rest of the simulation duration for both the pre and post-turbine configurations. Both the pre-turbine and post-turbine configurations feature a clean DPF.

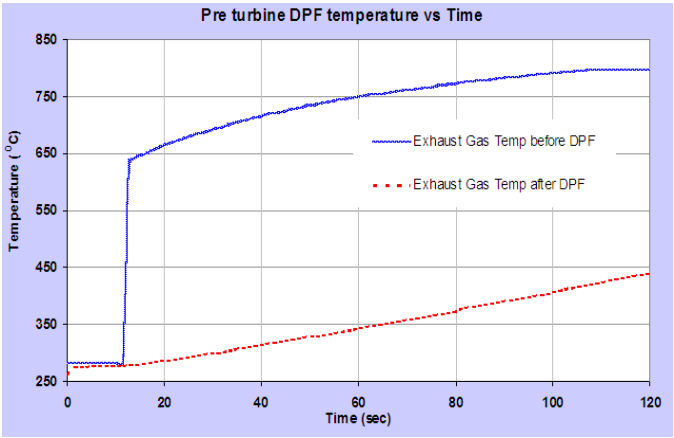

Figure 15: Pre-turbine DPF Temperature Distribution

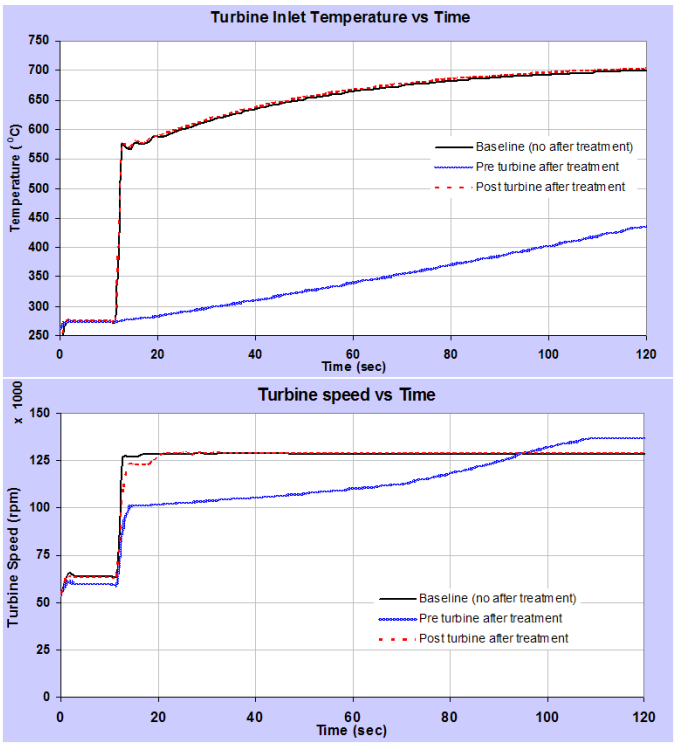

Figure 16: Comparison of Turbine Inlet Temperature and Speed

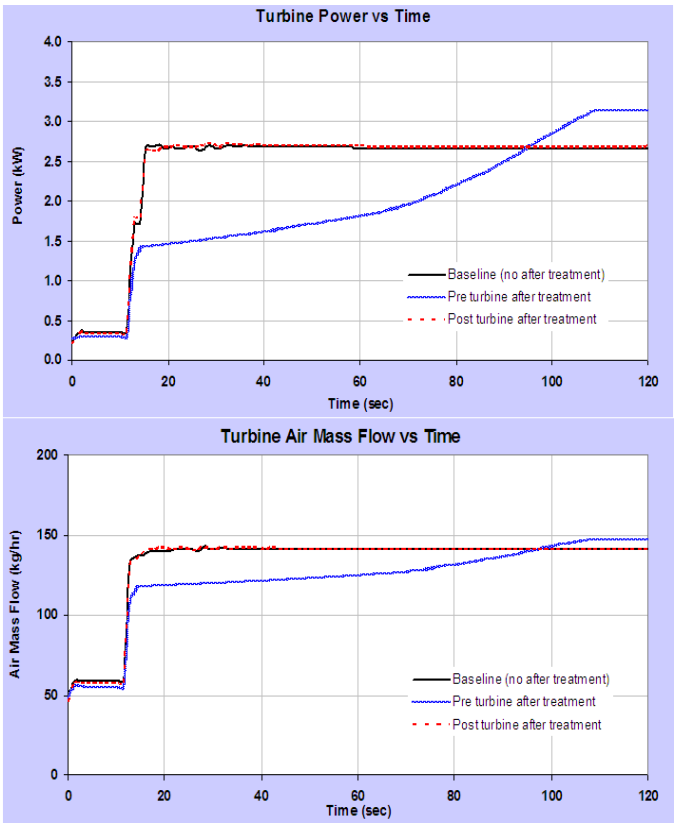

Figure 17: Comparison of Turbine Power and Mass Flow

The results clearly show that the post-turbine configuration has superior transient response. Figures 14 and 15 help explain the lackluster transient behavior observed with the pre-turbine configuration. In figure 15, during the load step, the DPF inlet temperature increases from 270 ^{0}C to 650 ^{0}C. However, due to its large thermal mass, DPF outlet temperature increases very slowly. This results in a very gradual increase in turbine inlet temperature and a similarly gradual build-up of turbine power. This translates directly into reduced engine mass air flow and BMEP. As the DPF outlet temperature increases, turbine power starts to increase. This gradually increases the boost and mass air flow allowing the BMEP to eventually reach its steady state value. Figure 16 compares the build up of turbine inlet temperature and turbocharger

rotational speed between both system configurations. Figure 17 provides a similar comparison of turbine power and engine mass air flow. The post-turbine configuration results in higher turbine outlet pressure as compared to the baseline configuration. This is the reason for the difference in turbine speed and power observed between the post-turbine and baseline configurations.

Transient simulations with DOC chemistry - Exothermic chemical reactions in the DOC increase its outlet gas temperature. This effect can improve the transient response of the pre-turbine after-treatment configuration. Load step simulations were performed for three distinct engine-out exhaust gas compositions listed below:

- No chemical reactions modeled in DOC
- Low HC and CO (300 ppm HC and 1000 ppm CO)
- Moderate HC and CO (600 ppm HC and 2000 ppm CO)
- High HC and CO (900 ppm HC and 3500 ppm CO)

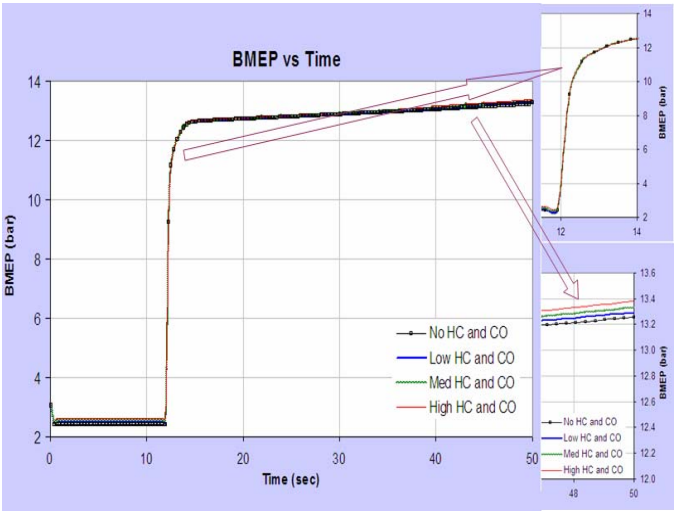

Figure 18: Load Steps with Varying Exhaust Composition

Results show that with an increase in exhaust CO and HC concentration, DOC outlet and DPF inlet temperatures increase as one would expect. However the large thermal inertia of the DPF dampens out this effect significantly, resulting in a minimal increase in DPF outlet temperature. The resulting turbine power gain is therefore very minor resulting in an equally minor gain in BMEP. Figure 18 shows the transient performance of the four cases studied. Figure 19 shows the effect of the chemical kinetics on the DOC outlet gas temperature. Figure 20 shows the DPF outlet temperature history and subsequent minor impact on turbine power as described above.

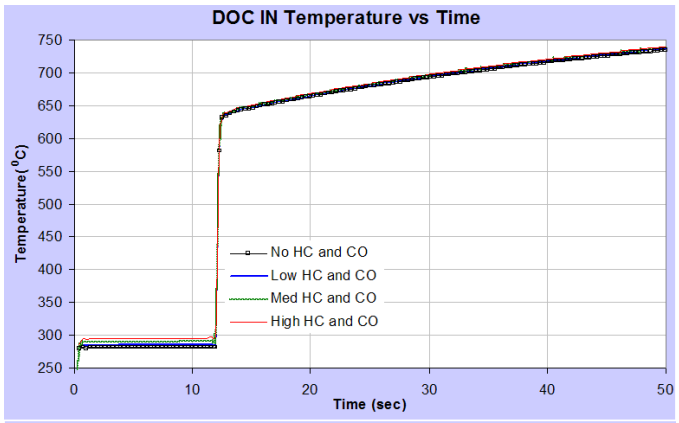

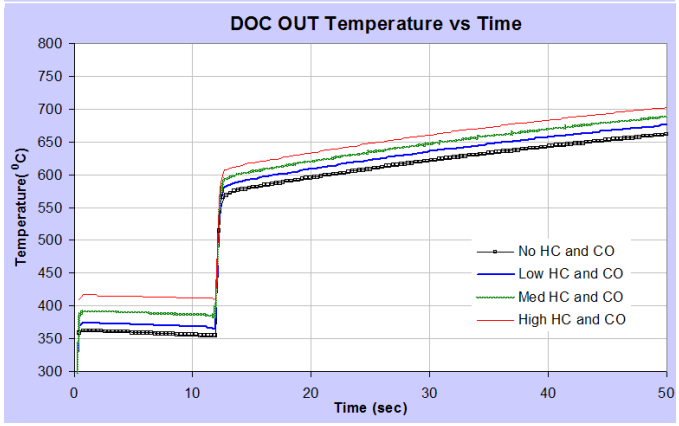

Figure 19: DOC Inlet and Outlet Temperature

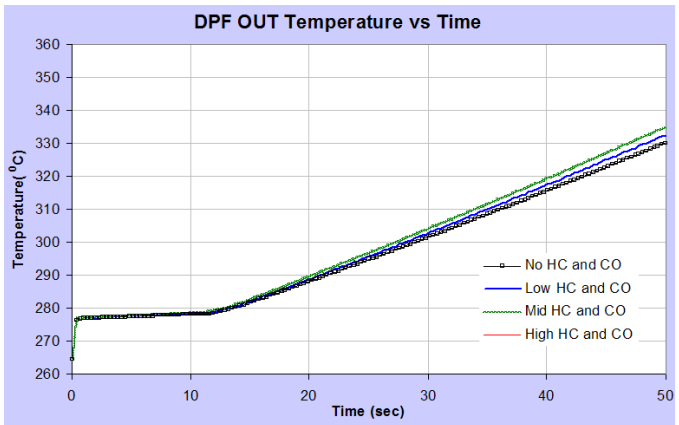

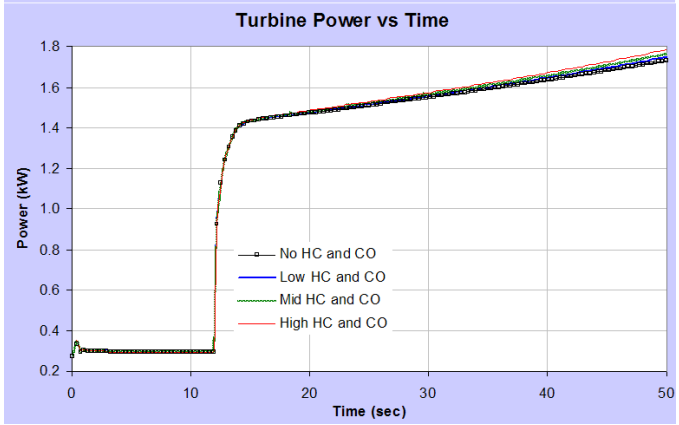

Figure 20: DPF Outlet Temperature and Turbine Power

CONCLUSIONS

This study illustrated that operating a diesel engine under steady-state conditions showed that fuel economy is significantly improved for a pre-turbo configured after-treatment system as opposed to a post-turbo variation. The reduction in pumping losses for a given BMEP can provide a higher availability of power, or an increase in fuel efficiency, while enabling an equivalent power output as a post-turbo system. Two major physical phenomena are present in these after-treatment systems that can provide this behavior. First, a post-turbo setup suffers from a significant reduction in the expansion ratio, by its placement within the exit path of the exhaust gas turbine. This produces a multiplying effect on the engine back pressure required to maintain a target boost pressure. Secondly, a post-turbo setup results in an aggravated pressure drop at the same physical loading level of the DPF. The pressure drop occurs because the density of the exhaust gas is lower after the turbine than before it. Pre-turbo after-treatment enables the possibility of downsizing the DPF, or over-boosting to provide increased torque output or EGR. The efficiency of the turbocharger needs to be included to have a complete understanding of its benefits. Boost pressure is not impacted over time by a pre-turbo after-treatment system; however, it does increases gas exchange losses that in turn reduce power availability on a brake basis. In contrast, a post-turbo after-treatment system experiences degradation in boost pressure degradation over time, which requires VGT compensation to maintain boost. The VGT compensation increases gas exchange losses that eventually cause a torque reduction. In an after-treatment system with a clean DPF or a system with limited restrictions, this advantage in the configuration is minor, particularly at low engine speeds and loads.

The analysis revealed that when operated under transient conditions, the pre-turbo DPF system showed a disadvantage in response. The placement of the DPF in a pre-turbo configuration causes it to act as a thermal absorber, which decreases the available for the turbine during transient operating conditions. Conversely, a post-turbo DPF does not receive the exhaust gas until it has already expanded through the turbine, which assists in its avoiding this thermal absorber effect. Transient behavior can be enhanced by positive exotherms created by the chemical oxidation processes that occur in the DOC. The net benefit of this impact is small, due to the large thermal mass of the DPF that dominates the problem during transients. It is expected that in the future, the mass of the substrate mass is expected to drop significantly, which will reduce the impact of the thermal absorber effect. Through a reduction in oil consumption and the use of ash free oil, a pre-turbine configuration can utilize a smaller DPF than that of a post-turbine system. These changing circumstances can also help reduce the thermal lag experienced by pre-turbine versions.

ACKNOWLEDGMENTS

The authors would like to thank BorgWarner Inc. and NGK, for data that was supplied for model correlation and validation. The authors also gratefully acknowledge financial assistance provided by BorgWarner for this work.

.

REFERENCES

1. Hirose, S., Yamamoto, Y., Miyairi, Y., Makino, M., Nakasuji, Y., Miwa, S., “Application of Converter Efficiency Simulation Tool for Substrate Design,” SAE Technical Paper No. 2004-01-1487.
2. Mizutani, Y., Watanabe, Y., Yuuki, K., Hashimoto, S., Hamanaka, T., Kawashima, J., “Soot Regeneration Model for SiC-DPF System Design,” SAE Technical Paper No. 2004-01-0159.
3. Haralampous, O.A., Koltsakis, G.C., Samaras, Z.C., Vogt, C.-D., Ohara, E., Watanabe, Y., Mizutani, T., “Reaction and Diffusion Phenomena in Catalyzed Diesel Particulate Filters,” SAE Technical Paper No. 2004-01-0696.
4. Haralampous, O.A., Koltsakis, G.C., Samaras, Z.C., Vogt, C.-D., Ohara, E., Watanabe, Y., Mizutani, T., “Modeling and Experimental Study of Uncontrolled Regenerations in SiC Filters with Fuel Borne Catalyst,” SAE Technical Paper No. 2004-01-0697.
5. Joergl, Volker, Mueller-Haas, Klaus, “Influence of pre-turbo catalyst design on diesel engine performance, emissions, and fuel economy,” SAE Technical Paper No. 2008-01-0071.
6. Mansour, Masoudi, “Pressure Drop of Segmented Diesel Particulate Filters,” SAE Technical Paper No. 2005-01-0971.

CONTACT

Mark Subramaniam
FEV, Inc.
subramaniam@fev-et.com